



# Mechanosensation is evolutionarily tuned to locomotor mechanics

Brett R. Aiello<sup>a</sup>, Mark W. Westneat<sup>a,b</sup>, and Melina E. Hale<sup>a,1</sup>

<sup>a</sup>Department of Organismal Biology and Anatomy, University of Chicago, Chicago, IL 60637; and <sup>b</sup>Division of Fishes, Field Museum of Natural History, Chicago, IL 60605

Edited by David B. Wake, University of California, Berkeley, CA, and approved February 24, 2017 (received for review October 10, 2016)

**The biomechanics of animal limbs have evolved to meet the functional demands for movement associated with different behaviors and environments. Effective movement relies not only on limb mechanics but also on appropriate mechanosensory feedback. By comparing sensory ability and mechanics within a phylogenetic framework, we show that peripheral mechanosensation has evolved with limb biomechanics, evolutionarily tuning the neuro-mechanical system to its functional demands. We examined sensory physiology and mechanics of the pectoral fins, forelimb homologs, in the fish family Labridae. Labrid fishes exhibit extraordinary morphological and behavioral diversity and use pectoral fin-based propulsion with fins ranging in shape from high aspect ratio (AR) wing-like fins to low AR paddle-like fins. Phylogenetic character analysis demonstrates that high AR fins evolved independently multiple times in this group. Four pairs of species were examined; each included a plesiomorphic low AR and a high AR species. Within each species pair, the high AR species demonstrated significantly stiffer fin rays in comparison with the low AR species. Afferent sensory nerve activity was recorded during fin ray bending. In all cases, afferents of stiffer fins were more sensitive at lower displacement amplitudes, demonstrating mechanosensory tuning to fin mechanics and a consistent pattern of correlated evolution. We suggest that these data provide a clear example of parallel evolution in a complex neuromechanical system, with a strong link between multiple phenotypic characters: pectoral fin shape, swimming behavior, fin ray stiffness, and mechanosensory sensitivity.**

neuromechanics | mechanosensation | evolution | locomotion | Labridae

The appendages of animals, from insect wings to tetrapod limbs, have evolved and diversified with the functional demands associated with a species' behaviors and the environments in which it lives (1–4). Whereas the evolution of appendage structure and movement has been identified as critical, both to key evolutionary innovations and to more subtle taxonomic specialization (1–3, 5, 6), it is clear that mechanosensation, which includes the ability to sense the relative movement and position of one's own body elements, is also critical for effective appendage function and control. For example, people who have lost mechanosensation of their limbs must attend visually to their affected limbs to know where they are in space and to modulate motor output effectively (7, 8). Experimental sensory denervation of limbs (9–12) and other appendages (13–15) in a range of other species has also been shown to result in significant disruption of normal movement. The recent discovery of mechanosensation in the pectoral fins of fishes (15–17) provides an opportunity to explore evolutionary patterns of mechanosensation relative to interspecific variation in limb locomotor biomechanics.

Sensory capabilities evolve with behavior to reflect the diverse sensory needs across species (18–20). The absolute range of perceptible sensory cues varies among species for a given sensory modality, as seen in the diversity of auditory frequency ranges represented among insects (18, 21) and rodents (22–24), and the olfactory detection thresholds among primates (25, 26). In addition, activity in particular regions of a sensory range may be enhanced to reflect biologically relevant inputs. For example, the

olfactory system has been highly specialized through evolution to the relevant olfactory cues (27–29). Appendage mechanosensation is different from these sensory modalities in that the appendages of animals are integrated sensorimotor structures that perform dual roles, acting as both sensory and motor structures during a given behavior (16, 30). Interspecific variation in appendage mechanics will influence the magnitude of bending and shape change incurred from the application of forces during locomotion (31, 32), which will consequently change the range of mechanosensory stimuli relevant to each species. The diversity of pectoral fin shape and behavior among fishes provides a unique opportunity to test whether the mechanosensory system undergoes correlated changes in relation to the mechanical properties of locomotor appendages, which would suggest that limb mechanics and the limb's associated mechanosensory system are major axes of structural and functional variation in neuromechanical systems.

In this study, we investigated the correlated evolution of mechanosensation and limb mechanics in fish pectoral fins, the homologs of tetrapod forelimbs. Pectoral fin nerves have recently been shown to provide feedback on fin ray bending amplitude and rate as well as on fin ray position (15, 16). Here we examined proprioception in the fish family Labridae (wrasses), a group that demonstrates considerable morphological, biomechanical, and movement diversity (33). Aspect ratio (AR) is a measure of the fin's span squared relative to its surface area, with higher AR indicating relatively longer and narrower, more wing-like fins, and low AR indicating a broader more paddle-like fin shape. Labrids use pectoral fin-based swimming behaviors along a continuum that

## Significance

**This paper provides an analysis of the correlated evolution of limb biomechanics and mechanosensation. We found that in multiple independent evolutions of stiff fins there was concurrent evolution of increased mechanosensory afferent sensitivity to low amplitude bends, compared with the nerve responses of more flexible fins. These results indicate that sensory systems are tuned to fin mechanical properties, revealing that limb mechanics and the limb's associated mechanosensory system are a new and important axis of structural and functional variation in locomotor systems. Further, we find high levels of parallelism between swimming behavior, fin shape, mechanics, and mechanosensation across a rich phylogeny of fishes, suggesting that neuromechanical tuning may be a general feature of evolution in neuromechanical systems.**

Author contributions: B.R.A., M.W.W., and M.E.H. designed research, performed research, analyzed data, and wrote the paper.

The authors declare no conflict of interest.

This article is a PNAS Direct Submission.

Data deposition: The sequences reported in this paper have been deposited in the GenBank database (accession nos. provided in Dataset S1). Aspect ratio sources and data, mechanical property data, electrophysiology data and phylogenetic tree files have been deposited in the Dryad Digital Repository (<http://dx.doi.org/10.5061/dryad.0463n>).

<sup>1</sup>To whom correspondence should be addressed. Email: [mhale@uchicago.edu](mailto:mhale@uchicago.edu).

This article contains supporting information online at [www.pnas.org/lookup/suppl/doi:10.1073/pnas.1616839114/-DCSupplemental](http://www.pnas.org/lookup/suppl/doi:10.1073/pnas.1616839114/-DCSupplemental).

ranges from drag-based rowing with broad, low AR fins for high maneuverability, to lift-based flapping driven by high AR, wing-like fins that maximize thrust and mechanical efficiency (33–37). The central aim of this study is to test the hypothesis that the mechanosensory response to fin ray bending undergoes evolutionary tuning with fin mechanical properties across a diversity of fin shapes and behaviors. First, we hypothesized that high AR pectoral fins have increased overall flexural stiffness due to their propensity to bend less during locomotion in comparison with more flexible low AR fins (Fig. S1). Second, we hypothesized that in comparison with more flexible fins, the reduced bending magnitude that occurs in stiff fins has driven their associated sensory system to evolve increased sensitivity to lower amplitude bending.

We sought to explore broad evolutionary patterns of fin design and function. To test our hypotheses in a phylogenetic framework, we performed a phylogenetic analysis of pectoral fin aspect ratio using a new phylogeny of 340 species of Labridae (Fig. 1 and Fig. S2). Based on this reconstruction, four species pairs were chosen, each pair from a different labrid subfamily. Within each pair, selected species used fins of divergent shapes, one with high AR fins and one with low AR fins. The four species pairs (*Gomphosus varius* and *Halichoeres bivittatus*, *Halichoeres hortulanus* and *Halichoeres melanurus*, *Scarus taeniopterus* and *Cheilinus fasciatus*, and *Clepticus parrae* and *Bodianus rufus*, high AR and low AR, respectively) were used to test patterns of correlated evolution between fin ray flexural stiffness and the mechanosensory afferent response to step-and-hold stimuli in our analysis of the evolutionary tuning of neuromechanical systems.

## Results

**Phylogenetics and Ancestral State Reconstruction.** Our analysis of DNA sequence data for 340 species of labrid fishes yielded a well-resolved phylogeny (Fig. S1) to use in exploring phylogenetic patterns of pectoral fin shape. Character optimization and ancestral state reconstruction revealed a most likely ancestral state of low AR fins at the root node of the tree (likelihood probabilities of each fin AR: low = 0.47, intermediate = 0.29, and high = 0.24) and at least 22 independent evolutions of high aspect ratio fins associated with the flapping swimming behavior (Fig. 1, Figs. S2 and S3, and Table S1). The phylogenetic reconstruction shows a rich history of fin shape evolution, with multiple clades having evolved upward and downward on the fin aspect ratio continuum, producing complex patterns of divergence and parallelism across the tree. High AR fins (AR > 3.2) were highly significantly ( $P < 0.01$ ) convergent across the tree. Whereas the character state at the root node is equivocal, ancestral state reconstructions show high likelihood values for character states of low, intermediate, or high AR at progressively more distal nodes. Therefore, our interpretation of multiple independent evolutions of high aspect ratio fins is not dependent on the character state at the root node. The probability of representing the low AR character state at the node of a species pair's most recent common ancestor is 0.872 for *C. parrae* and *B. rufus* (node 27), 0.756 for *G. varius* and *H. bivittatus* (node 206), and 0.750 for *H. melanurus* and *H. hortulanus* (node 296). The node (node 58) of the most recent common ancestor between *C. fasciatus* and *S. taeniopterus* has a 0.491 probability of representing the low AR fin character state. Although this node is equivocal, the parrotfish *S. taeniopterus* represents a large clade of high AR flapping species, and a particularly notable independent evolution of high aspect ratio fins from the common ancestor of the cheiline and scarine wrasses.

**Fin Ray Mechanics.** The morphological phenotypes of low and high AR fins (Fig. 2A) corresponded to a strong divergence in fin ray flexural stiffness. The average flexural stiffness, or resistance to bending, at 50% fin ray length was between  $190 \pm 30$  and  $210 \pm 50 \times 10^{-9} \text{ N}\cdot\text{m}^2$  (average  $\pm$  SD) among the high AR species and between  $20 \pm 10$  and  $40 \pm 10 \times 10^{-9} \text{ N}\cdot\text{m}^2$  among the low AR

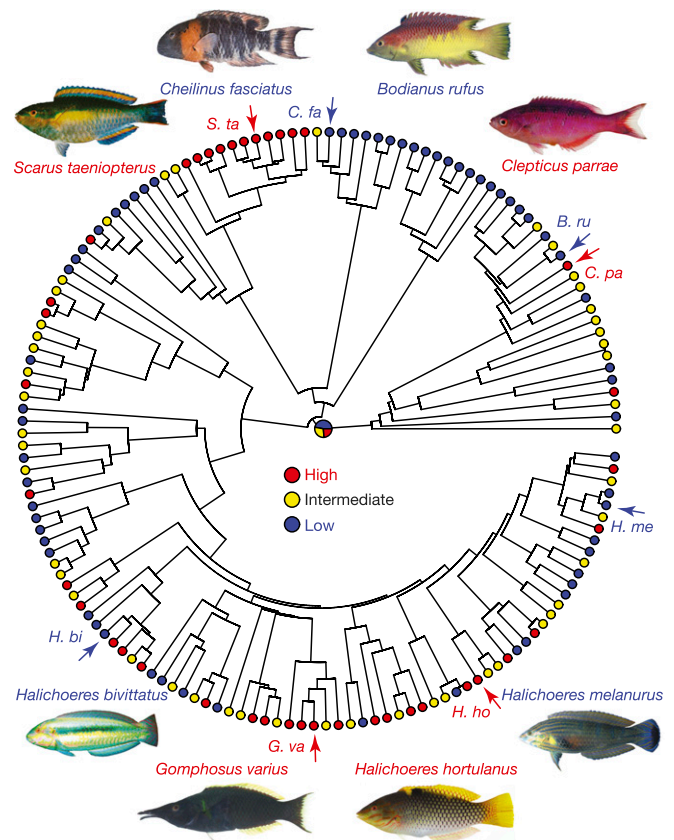


**Fig. 1.** The phylogenetic relationships of the Labridae and pectoral fin aspect ratio ancestral state reconstruction. The maximum likelihood reconstruction revealed a most likely ancestral state of low aspect ratio pectoral fins (low = 0.47, intermediate = 0.29, high = 0.24) and at least 22 independent evolutions of high aspect ratio fins. An arrow and the species' initials highlights the phylogenetic position of each species used in this study. The two species of each pair were always located within the same subfamily and each species pair contains an independent evolution of the high AR fin. The phylogeny presented here is pruned from 340 species to 150 species to maximize visualization. The ancestral state of the basal node is taken from the 340 species reconstruction. The full 340 species phylogeny and accompanying 340 species ancestral state reconstruction can be found in Fig. S2, and the node labels and the corresponding likelihood of the ancestral state at each node can be found in Fig. S3 and Table S1, respectively. Red, high aspect ratio; yellow, intermediate aspect ratio; and blue, low aspect ratio. Photo credits: *H. bivittatus*, Paul Humann; *H. hortulanus* and *G. varius*, Jeffrey T. Williams; and *B. rufus*, *C. parrae*, *C. fasciatus*, *H. melanurus*, and *S. taeniopterus*, John E. Randall.

species. These data indicate largely consistent trends in flexural stiffness among size-matched individuals in each behavioral phenotype. Within each species pair, the average flexural stiffness at 50% fin ray length of high AR fins was 5.4–11.6 times greater and significantly different from that of low AR fins (Fig. 2B;  $t$  test  $P$  values  $< 0.05$ ; Fig. S4). Across all eight species, flexural stiffness decreases exponentially along the length of the fin ray, and regressions of stiffness against fin ray position reveal significant differences in the  $y$  intercept between species for all four pairs and significant differences in the regression slope between species for three pairs (*G. varius* and *H. bivittatus*, *C. parrae* and *B. rufus*, and *C. fasciatus* and *S. taeniopterus*) ( $P < 0.01$ ; Table S2). The significant differences in  $y$  intercept suggest that there is a strong species effect on fin ray stiffness and significant differences in the regression slope suggest that the rate fin ray stiffness changes along the length of the fin ray is different between species.

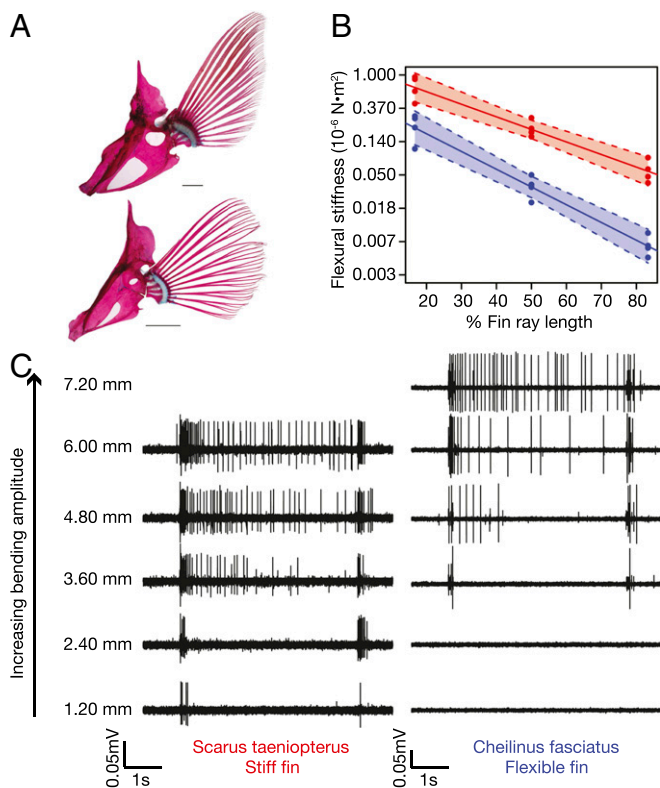


**Fig. 2.** Comparative pectoral fin morphology, mechanics, and proprioceptive sensitivity between closely related low AR (*C. fasciatus*) and high AR (*S. taeniopterus*) species. (A) Cleared and stained pectoral fins of *S. taeniopterus* (flapper; Top) and *C. fasciatus* (rower; Bottom). *S. taeniopterus* employs wing-like high-aspect ratio pectoral fins, whereas *C. fasciatus* employs broad paddle-like pectoral fins. (Scale bars, 1 cm.) (B) The pectoral fin rays of *S. taeniopterus* (high AR; red) are significantly stiffer than the rays of *C. fasciatus* (low AR; blue). All flexural stiffness data for each species were pooled and fit with an exponential curve ( $r^2 = 0.93, 0.95$  for *S. taeniopterus* and *C. fasciatus*, respectively). Correspondingly, the data are presented in a semilog fashion with a logarithmically scaled y axis. The shaded region of each fit represents a 99% confidence interval of the linear regression. The y intercept and slope of the regression line was significantly different between each species ( $P < 0.05$ ; Table S2). (C) Representative nerve recordings from one individual of *S. taeniopterus* (Left) and *C. fasciatus* (Right). A three times larger bending magnitude is needed to elicit a response in the size-matched pectoral fin of the flexible-finned *C. fasciatus* in comparison with the stiff-finned *S. taeniopterus*.

**Mechanosensation.** Afferent nerve responses to fin ray bending were recorded for all eight of the species tested and consistent trends were identified among taxa. In response to step-and-hold stimuli, where a single fin ray is bent, held in a bent position, and then returned to rest, a burst of spikes occurred both when the fin was raised from and when it was returned to its resting position. The duration of bursts (three or more spikes within 50 ms of each other) associated with stimulus onset increased significantly with increasing bending amplitude (Fig. 3A and Table S3). Furthermore, fibers continued to respond during the hold phase of the stimulus (Fig. 2C). At high bending amplitudes, the spike rate over the hold period (a 3-s portion of the trace that began 1.5 s after stimulus onset to ensure activity associated with fin movement was not included in this analysis) was significantly greater than the spike rate of a prestimulus baseline for each species used in this study (one-way ANOVAs,  $P < 0.05$ ; Table S4). At these higher bending amplitudes, a significant and positive relationship was found between hold period spike rate and bend amplitude ( $P < 0.05$ ) for all individuals across all species (Fig. S5 and Table S5).

Comparing across the species pairs, stiff-finned species consistently demonstrated greater sensitivity in comparison with species using more flexible fins. The average minimum bending amplitude to elicit a response (response threshold) was between  $17.84 \pm 0.88$  and  $30.67 \pm 1.03\%$  fin ray length ( $3.6 \pm 0.0$  and  $6.12 \pm 0.72$  mm) among the low AR species and between  $5.91 \pm 0.58$  and  $8.20 \pm 3.03\%$  fin ray length ( $1.05 \pm 0.3$  and  $1.5 \pm 0.42$  mm) among the high AR species (Table S6). Similar to fin stiffness, these data show consistent trends in response threshold among size-matched individuals in each morphological phenotype. Within each species pair, the average response threshold of the low AR species was 2.39–5.19 times greater in percent fin ray length than that of the high AR species (Fig. 3B). This finding corresponds to differences in average response threshold between the species of each pair ranging from approximate bending magnitudes of 11–25% fin ray length and significant differences in response thresholds between the species of each pair ( $P < 0.0125$ ; Fig. 3A). Furthermore, the slope of the

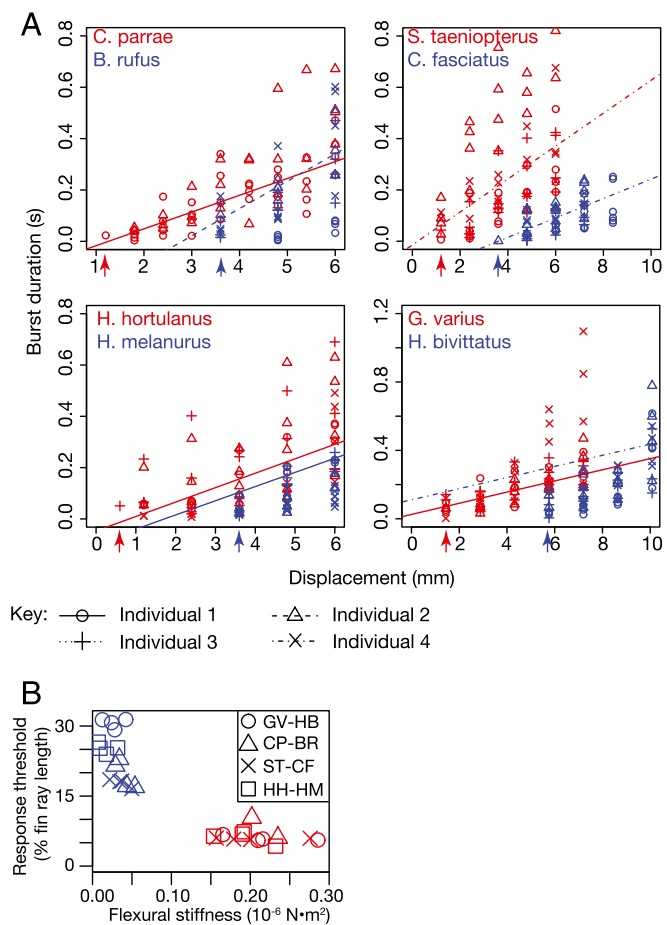


**Fig. 3.** Summary of afferent response to fin ray bending. (A) Bivariate plots of burst duration by fin ray bending magnitude per species. The duration of bursts (three or more spikes within 50 ms of each other) associated with the onset of fin ray movement is positively and significantly correlated with fin ray bending magnitude. Regression lines are presented for one representative individual of each species, and regression statistics for all individuals are detailed in Table S3. Arrows represent minimum response amplitude per species. (B) Response threshold (the minimum bending amplitude needed to elicit a response) is plotted against fin ray flexural stiffness for every individual of each species. In all cases, the pectoral fin rays of high AR fins are significantly stiffer than those of low AR fins, and the proprioceptive system of high AR species is significantly more sensitive than that of low AR species. Blue, flexible low AR fins; red, stiff high AR fins.



In an evolutionary context, the phylogenetic analysis of fin shape reveals strong evidence of parallel evolution across the tree topology. In this study, we focused on 4 of the 22 known independent evolutions of high AR pectoral fins (Fig. 1 and Fig. S2). In each of these 4 cases, high AR pectoral fins evolved in parallel from a similar low AR ancestor, and this same pattern is seen repeatedly across the tree topology (Fig. S1). In all 4 independently evolving species pairs, pectoral fin mechanics evolve in tandem with AR, and as fins evolve increased stiffness, the sensitivity of their mechanosensory system also increases. The close association between swimming behavior (33) and biomechanics (34–36) with pectoral fin shape in these fishes suggests that the mechanosensory system has coevolved with the anatomical and behavioral diversification of the labrid fishes. We suggest that this is a clear example of parallel evolution in a complex neuromechanical system, with a strong link between multiple phenotypic characters: pectoral fin shape, swimming behavior, fin ray stiffness, and mechanosensory sensitivity. Further exploration of mechanosensation in this system, focused on species with a diversity of fin shapes, may yield information on the function of the mechanosensory system in intermediate forms and the role that sensory neuromechanics plays in driving evolutionary trends in locomotor diversity.

Broadly across animals, a spectacular morphological and biomechanical diversity of appendages are used in a vast repertoire of behaviors. The locomotor appendages of animals, from insect wings to vertebrate limbs, perform dual roles as sensors and propulsors (16, 49, 50). We argue that the diversification of locomotor appendages involves the evolutionary tuning of mechanosensation to the concurrent evolutionary changes in the material and morphological properties of propulsors (wings, fins, and limbs). This study demonstrates that the mechanosensory system has evolved to meet the dynamic range of fin movement in multiple independently evolving pairs of closely related fishes. The broad sampling of our study demonstrates that, as the fin evolves increased stiffness, the sensory system evolves increased sensitivity. These results suggest that the correlated evolution of the mechanosensory system and appendage biomechanics is a general principle of how neuromechanical systems evolve. As mechanosensation is a universal feature of organisms (51), neuromechanical tuning may be an evolutionary principle that shapes the functional capabilities of all animals.

## Materials and Methods

Species pairs were selected from the phylogenetic topology specifically to be close relatives with divergent fin shapes, representing disparate regions of the tree. Four adult *G. varius* (9.9–12.0 cm), *H. bivittatus* (8.0–10.9 cm),

*H. hortulanus* (7.3–10.5 cm), *H. melanurus* (7.5–8.8 cm), *C. fasciatus* (9.5–13.2 cm), *S. taeniopterus* (9.5–11.9 cm), and *B. rufus* (7.8–10.2 cm) and two adult *C. parrae* (8.1 and 8.2 cm) were used in this study. There were no significant differences in size between the individuals of the two species in each pair ( $P > 0.05$ ). Two additional *H. bivittatus* were used in this study to expand the range of body sizes (standard lengths: 5.3 and 16.2 cm).

A phylogenetic analysis of 340 species of labrid fishes was performed, using an aggregated dataset of 10 genes used in previous labrid phylogenetics (52, 53), new sequences generated for this study, and additional genetic data obtained from GenBank (Dataset S1). Pectoral fin aspect ratio character states for 340 species were visualized at the tips of the phylogeny and analyzed using likelihood ancestral state reconstructions using the R packages ape (54) and phytools (55). Pectoral fin aspect ratio was calculated as the square of the longest fin span (usually the leading edge), divided by fin area. Aspect ratio was binned into three discrete characters: low AR (AR: 0.73–1.5), intermediate AR (AR: 1.50–3.0), and high AR (AR: 3.0–4.6).

For each animal used, we performed mechanical testing in one pectoral fin and the physiological recording of the afferent response to fin bending in its pair. Intrinsic pectoral fin ray flexural stiffness was measured through a series of three point bending tests along the ray's span with a material testing machine (LS1, Lloyd Instruments) using a 50 N load cell. We recorded from pectoral fin nerves following published methods (16). An extracellular glass suction electrode was connected to one of the afferent nerve fibers to record multiunit physiological responses to fin ray bending. The fin rays were clamped at their proximal end and the interray membrane was cut to isolate the individual ray for bending. Randomly ordered series of step-and-hold stimuli were applied to the third fin ray of each individual. Data were analyzed in MATLAB 7.10.0 (Mathworks) using a custom routine (R. Williams IV, University of Chicago). The burst duration associated with the stimulus onset (fin movement) and the spike rate over the hold period of the stimulus were calculated. All statistical analyses were performed in RStudio 0.98.484 (RStudio, Inc.) or JMP 9.0.1 (SAS). All experimental procedures were carried out under University of Chicago Institutional Animal Care and Use Committee guidelines (protocol 71589 to M.E.H.). The unabridged materials and methods section can be found as [SI Materials and Methods](#).

**ACKNOWLEDGMENTS.** We thank Richard Williams IV, Callum Ross, Sliman Bensmaia, Michael LaBarbera, Michael Coates, Adam Hardy, Hilary Katz, Thomas Stewart, Aaron Olsen, Timothy Sosa, Katharine Henderson, and Dallas Krentzel for helpful discussion and/or feedback on the manuscript; Adam Hardy and Chery Cherian for help collecting some of the mechanical property data; the many colleagues and institutions that have shared labrid tissue samples and specimens; Lydia Smith, Jillian Hens, Charlene McCord, and others involved in DNA sequencing; and Evan Koch for invaluable advice and help with statistical analyses. This work was supported by the National Science Foundation under grants DGE-0903637 (a traineeship that supported B.R.A.), IOS 1425049 and DEB 1541547 (to M.W.W.), and IOS 1257886 (to M.E.H.); and the Office of Naval Research under Grant N00014-0910352 (to M.E.H.). Funding also came from the University of Chicago through the Hinds Fund (B.R.A.).

- Gillis GB, Blob RW (2001) How muscles accommodate movement in different physical environments: Aquatic vs. terrestrial locomotion in vertebrates. *Comp Biochem Physiol A Mol Integr Physiol* 131:61–75.
- Higham TE, Birn-Jeffery AV, Collins CE, Hulsey CD, Russell AP (2015) Adaptive simplification and the evolution of gecko locomotion: Morphological and biomechanical consequences of losing adhesion. *Proc Natl Acad Sci USA* 112:809–814.
- Losos JB (1990) Ecomorphology, performance capability, and scaling of West-Indian anolis lizards: An evolutionary analysis. *Ecol Monogr* 60:369–388.
- Wootton RJ (1992) Functional morphology of insect wings. *Annu Rev Entomol* 37:113–140.
- Bellwood DR, Wainwright PC (2001) Locomotion in labrid fishes: Implications for habitat use and cross-shelf biogeography on the Great Barrier Reef. *Coral Reefs* 20:139–150.
- Pierce SE, Clack JA, Hutchinson JR (2012) Three-dimensional limb joint mobility in the early tetrapod *Ichthyostega*. *Nature* 486:523–526.
- Sainburg RL, Poizner H, Ghez C (1993) Loss of proprioception produces deficits in interjoint coordination. *J Neurophysiol* 70:2136–2147.
- Sanes JN, Mauritz KH, Dalakas MC, Evars EV (1985) Motor control in humans with large-fiber sensory neuropathy. *Hum Neurobiol* 4:101–114.
- Abelew TA, Miller MD, Cope TC, Nichols TR (2000) Local loss of proprioception results in disruption of interjoint coordination during locomotion in the cat. *J Neurophysiol* 84:2709–2714.
- Gray J, Lissmann HW (1940) The effect of deafferentation upon the locomotor activity of amphibian limbs. *J Exp Biol* 17:227–237.
- Tourtellotte WG, Milbrandt J (1998) Sensory ataxia and muscle spindle agenesis in mice lacking the transcription factor *Egr3*. *Nat Genet* 20:87–91.
- Woo SH, et al. (2015) Piezo2 is the principal mechanotransduction channel for proprioception. *Nat Neurosci* 18:1756–1762.
- Hall JM, et al. (2015) Kinematic diversity suggests expanded roles for fly halteres. *Biol Lett* 11:20150845.
- Sane SP, Dieudonné A, Willis MA, Daniel TL (2007) Antennal mechanosensors mediate flight control in moths. *Science* 315:863–866.
- Williams R 4th, Hale ME (2015) Fin ray sensation participates in the generation of normal fin movement in the hovering behavior of the bluegill sunfish (*Lepomis macrochirus*). *J Exp Biol* 218:3435–3447.
- Williams R 4th, Neubarth N, Hale ME (2013) The function of fin rays as proprioceptive sensors in fish. *Nat Commun* 4:1729.
- Hardy AR, Steinworth BM, Hale ME (2016) Touch sensation by pectoral fins of the catfish *Pimelodus pictus*. *Proc Biol Sci* 283:20152652.
- Moir HM, Jackson JC, Windmill JF (2013) Extremely high frequency sensitivity in a 'simple' ear. *Biol Lett* 9:20130241.
- Simoncelli EP, Olshausen BA (2001) Natural image statistics and neural representation. *Annu Rev Neurosci* 24:1193–1216.
- Warrant E (2004) Vision in the dimmest habitats on earth. *J Comp Physiol A Neuroethol Sens Behav Physiol* 190:765–789.
- Cardone B, Fullard JH (1981) Auditory characteristics and sexual dimorphism in the gypsy moth. *Physiol Entomol* 13:9–14.
- Plassmann W, Kadel M (1991) Low-frequency sensitivity in a gerbilline rodent, *Pachyuromys duprasi*. *Brain Behav Evol* 38:115–126.
- Webster DB, Webster M (1971) Adaptive value of hearing and vision in kangaroo rat predator avoidance. *Brain Behav Evol* 4:310–322.
- Webster DB, Webster M (1972) Kangaroo rat auditory thresholds before and after middle ear reduction. *Brain Behav Evol* 5:41–53.

25. Laska M, Seibt A, Weber A (2000) 'Microsmatic' primates revisited: Olfactory sensitivity in the squirrel monkey. *Chem Senses* 25:47–53.
26. Passe DH, Walker JC (1985) Odor psychophysics in vertebrates. *Neurosci Biobehav Rev* 9:431–467.
27. Andersson MN, Larsson MC, Schlyter F (2009) Specificity and redundancy in the olfactory system of the bark beetle *Ips typographus*: Single-cell responses to ecologically relevant odors. *J Insect Physiol* 55:556–567.
28. Dekker T, Ibba I, Siju KP, Stensmyr MC, Hansson BS (2006) Olfactory shifts parallel superspecialism for toxic fruit in *Drosophila melanogaster* sibling, *D. sechellia*. *Curr Biol* 16:101–109.
29. Hansson BS, Stensmyr MC (2011) Evolution of insect olfaction. *Neuron* 72:698–711.
30. Muniak MA, Ray S, Hsiao SS, Dammann JF, Bensmaia SJ (2007) The neural coding of stimulus intensity: Linking the population response of mechanoreceptive afferents with psychophysical behavior. *J Neurosci* 27:11687–11699.
31. Gordon JE (1978) *Structures: Or Why Things Don't Fall Down* (Penguin Books, New York).
32. Vogel S (2003) *Comparative Biomechanics: Life's Physical World* (Princeton University Press, Princeton, NJ).
33. Wainwright PC, Bellwood DR, Westneat MW (2002) Ecomorphology of locomotion in labrid fishes. *Environ Biol Fishes* 65:47–62.
34. Walker JA, Westneat MW (2000) Mechanical performance of aquatic rowing and flying. *Proc Biol Sci* 267:1875–1881.
35. Walker JA, Westneat MW (2002) Kinematics, dynamics, and energetics of rowing and flapping propulsion in fishes. *Integr Comp Biol* 42:1032–1043.
36. Walker JA, Westneat MW (2002) Performance limits of labriform propulsion and correlates with fin shape and motion. *J Exp Biol* 205:177–187.
37. Westneat MW, Thorsen DH, Walker JA, Hale ME (2004) Structure, function, and neural control of pectoral fins in fishes. *IEEE J Oceanic Eng* 29:674–683.
38. Aiello BR, Stewart TA, Hale ME (2016) Mechanosensation in an adipose fin. *Proc Biol Sci* 283:20152794.
39. Petzold BC, Park SJ, Mazzochette EA, Goodman MB, Pruitt BL (2013) MEMS-based force-clamp analysis of the role of body stiffness in *C. elegans* touch sensation. *Integr Biol* 5:853–864.
40. Wang Y, Marshall KL, Baba Y, Lumpkin EA, Gerling GJ (2013) Natural variation in skin thickness argues for mechanical stimulus control by force instead of displacement. In World Haptics Conference. IEEE:645–650.
41. Krieg M, Dunn AR, Goodman MB (2015) Mechanical systems biology of *C. elegans* touch sensation. *BioEssays* 37:335–344.
42. Phelan C, Tangorra J, Lauder G, Hale M (2010) A biorobotic model of the sunfish pectoral fin for investigations of fin sensorimotor control. *Bioinspir Biomim* 5:035003.
43. Raibert MH (1986) *Legged Robots That Balance* (MIT Press, Cambridge, MA).
44. Kuo AD (2002) The relative roles of feedforward and feedback in the control of rhythmic movements. *Mot Contr* 6:129–145.
45. Galloway KC, Clark JE, Yim M, Koditschek DE (2011) Experimental investigations into the role of passive variable compliant legs for dynamic robotic locomotion. 2011 IEEE International Conference on Robotics and Automation:1243–1249.
46. Hurst J (2008) *The Role and Implementation of Compliance in Legged Locomotion* (Carnegie Mellon University, Pittsburgh, PA).
47. Galloway KC, Clark JE, Koditschek DE (2013) Variable stiffness legs for robust, efficient, and stable dynamic running. *J Mech Robot* 5:11009.
48. Elzinga MJ, Dickson WB, Dickinson MH (2012) The influence of sensory delay on the yaw dynamics of a flapping insect. *J R Soc Interface* 9:1685–1696.
49. Dickinson MH (1990a) Linear and nonlinear encoding properties of an identified mechanoreceptor on the fly wind measured with mechanical noise stimulation. *J Exp Biol* 151:219–244.
50. Dickinson MH (1990b) Comparison of the encoding properties of campaniform sensilla on the fly wing. *J Exp Biol* 151:245–261.
51. Kung C (2005) A possible unifying principle for mechanosensation. *Nature* 436:647–654.
52. Smith LL, Fessler JL, Alfaro ME, Strelman JT, Westneat MW (2008) Phylogenetic relationships and the evolution of regulatory gene sequences in the parrotfishes. *Mol Phylogenet Evol* 49:136–152.
53. Westneat MW, Alfaro ME (2005) Phylogenetic relationships and evolutionary history of the reef fish family Labridae. *Mol Phylogenet Evol* 36:370–390.
54. Paradis E, Claude J, Strimmer K (2004) APE: Analyses of Phylogenetics and Evolution in R language. *Bioinformatics* 20:289–290.
55. Revell LJ (2012) phytools: An R package for phylogenetic comparative biology (and other things). *Methods Ecol Evol* 3:217–223.
56. Schindelin J, et al. (2012) Fiji: An open-source platform for biological-image analysis. *Nat Methods* 9:676–682.
57. Arbuckle K, Bennett CM, Speed MP (2014) A simple measure of the strength of convergent evolution. *Methods Ecol Evol* 5:685–693.
58. Young WC, Budynas RG, Sadegh A (2012) *Roark's Formulas for Stress and Strain* (McGraw-Hill, New York), 8th Ed.
59. Blob RW, LaBarbera M (2001) Correlates of variation in deer antler stiffness: Age, mineral content, intra-antler location, habitat, and phylogeny. *Biol J Linn Soc Lond* 74:113–120.
60. Masino MA, Fetcho JR (2005) Fictive swimming motor patterns in wild type and mutant larval zebrafish. *J Neurophysiol* 93:3177–3188.